Comparative Transcriptomics Reveal Different Genetic Adaptations of Biofilm Formation in Bacillus subtilis isolate 1JN2 in Response to Cd2+ treatment

Wei Yang (yangw107@126.com)
Huaiyin Normal University https://orcid.org/0000-0003-1491-5108
Haixia Yan
Agro-Tech Extension and Service Center of Huai'an
Guanghui Dong
Huaiyin Normal University
Zhengpeng Li
Huaiyin Normal University
Chunhao Jiang
Nanjing Agricultural University
Dalu Gu
Huaiyin Institute of Agricultural Sciences of Xuhuai Region in Jiangsu
Dongdong Niu
Nanjing Agricultural University
Danni Zhou
Huaiyin Normal University
Yuming Luo
Huaiyin Normal University

Research Article

Keywords: Bacillus subtilis, Biofilm, Cadmium, Stress response, Adaptation, Transcriptomics analysis

Posted Date: April 15th, 2022

DOI: https://doi.org/10.21203/rs.3.rs-1402631/v1

Abstract

Biofilm plays important roles in the life cycle of *Bacillus* species, such as promoting host and object surface colonization and resisting heavy metal stress. This study utilized transcriptomics to evaluate the impacts of cadmium on the components, morphology, and function of the biofilms of *Bacillus subtilis* strain 1JN2. The morphology of the *B.subtilis* 1JN2 biofilm flattened, and its mobility increased under cadmium ion stress. Moreover, differential gene expression analysis showed that the main regulator of biofilm formation, Spo0A, decreased under cadmium ion stress, thereby inhibiting extracellular polysaccharides synthesis through the SinI/SinR two-component regulatory system and the AbrB pathway. Cadmium ion treatment also increased the SigD content significantly, thereby increasing the expression of the flagella encoding and assembly genes of the strain. This promoted poly-γ-glutamic acid production via the DegS/DegU two-component regulatory system and conversion of biofilm extracellular polysaccharide to poly-γ-glutamic acid. This conferred cadmium stress tolerance in the strain. Additionally, the cadmium ion-mediated changes in the biofilm composition did not affect the colonization of the host plant roots and biocontrol activity of the strain. Cadmium ions also induced surfactin synthesis by the strain. These findings illustrate the potential of *Bacillus* species as biocontrol strains that can help mitigate plant pathogenic infections and heavy metal stress. The results also provide a basis for the screening of multifunctional biocontrol strains.

Background

Biofilm plays an important role in the life cycle and existence of *Bacillus* in nature (Yang et al., 2018). It can protect the bacterium from environmental stress such as antibiotics (Høiby et al., 2010), and aid bacterial colonization of the host plant roots (Bais et al., 2004; Beauregard et al., 2013). The latter is considered the first and most important defense technique biocontrol agents use against soil-borne pathogens. Biofilm-enhanced mutants have been reported to exhibit enhanced biocontrol activities against *Ralstonia*, while biofilm-deletion mutants have reduced disease prevention capacity (Yang et al., 2018).

The regulatory pathway for biofilm formation is well-defined in *B.subtilis* (Vlamakis et al., 2013). Briefly, the environmental signals (like plant root secretions) are perceived by sensory histidine kinases (such as KinC/KinD), which activate the global master regulator, Spo0A, through protein phosphorylation (López et al., 2009; McLoon et al., 2011; Chen et al., 2012; Beauregard et al., 2013; Shemesh and Chai, 2013). The phosphorylated Spo0A (Spo0A-P) induces biofilm formation via two independent mechanisms which antagonize the two main repressors (SinR and AbrB), inhibiting biofilm formation (Hamon and Lazazzera, 2001; Chai et al., 2011).

Poly-γ-glutamic acid (γ-PGA), ranging from about 10 to 1000 kDA in size, is an important component of *B. subtilis* biofilm matrix (Morikawa et al., 2006; Poo et al., 2010; Ogunleye et al., 2015). Its biosynthesis in *B. subtilis* is regulated by the conserved operon *pgsB-pgsC-pgsA-pgsE* (previously named *ywsC-ywtA-ywtB-ywtC*) (Ashiuchi and Misono, 2002). These genes are highly conserved across different *Bacillus* species,

including *B. cereus* and *B. anthracis* (Ursu et al., 1989; Stanley and Lazazzera, 2005). In *B. subtilis*, the *pgs* operon is regulated by two cascades (ComA-ComP and DegS-DegU) of the two-component system (Stanley and Lazazzera, 2005).

Furthermore, γ-PGA biosynthesis may have interplay with the regulatory pathway of EPS (extracellular polysaccharides) production. Yu et al. (2016 reported that down-regulated expression of *epsD* and *yqxM*, responsible for biofilm formation, have minimal effects on the expression of γ-PGA synthesis gene *ywtB*. Contrarily, overproduction of γ-PGA in *B. amyloliquefaciens* C06 and its *epsA* and *tasA* mutants resulted in reduced EPS and TasA levels (Liu et al., 2010). Moreover, KinC and KinD negatively regulate γ-PGA production in *B.subtilis* by activating Spo0A, which down-regulates AbrB activities. Thus, this pathway positively regulates biofilm formation but negatively controls γ-PGA production, implying an interesting switch-like mechanism of the EPS and γ-PGA production. Conversely, the reverse regulatory pathway mediated by the DegS-DegU two-component system positively regulates γ-PGA production but strongly inhibits biofilm matrix genes (Yu et al., 2016).

Poly-γ-glutamic acid plays different roles in various *B.subtilis* isolates. Deleting *ywsAB* and *ywsC*, homologous to *pgsBCA*, resulted in weak biofilm formation in *B. subtilis* JH642; however, there were no differences in biofilm formation between *pgsBCA* mutant and the wild type strain of *B.subtilis* 3610 (Stanley and Lazazzera, 2005; Branda et al., 2006). Moreover, γ-PGA has been proven essential for *B. amyloliquefaciens* C06 and *B. subtilis* isolates colonization of apple (Liu et al., 2010) and tomato root surfaces (Yu et al., 2016), respectively.

Although the regulatory pathways of EPS production and γ-PGA biosynthesis have been well studied, the cause of their production shift is still unclear. It is also unknown whether changes between these two biofilm components might affect other activities, such as colonization and biocontrol ability of the implicated strains. This study utilized comparative transcriptomics to evaluate the impacts of cadmium on the components, morphology, and function of the biofilms of a *B.subtilis* strain 1JN2. The strain is an efficient biocontrol agent of *Ralstonia* (Yang et al., 2012) and could also alleviate Cd^{2+} stress in the host plant (Yang et al., 2015). We demonstrated that high concentrations of Cd^{2+} induced γ-PGA biosynthesis and inhibited EPS production in *B.subtilis* 1JN2. The shift between EPS and γ-PGA production enabled the strains to adapt to heavy metal contamination and persistently control host plant diseases.

Materials And Methods

Strains, Reagents, and Media Conditions

We used a wild *Bacillus subtilis* strain (1JN2), previously isolated by Yang et al. (2018), for the experiments. Competent 1JN2 strains containing chloramphenicol resistance were prepared and then electrotransformed with a green fluorescent plasmid (pGFP 4412) for fluorescent microscopy using the method by Xue (2008). All strains were routinely grown in Luria-Bertani (LB) broth (10 g/L of tryptone, 5

g/L of yeast extract, and 5/L g of NaCl) or LB medium with 1.5% agar. Conversely, biofilm formation was conducted using LBGM medium (LB + 1% (v/v) glycerol + 0.1 mM $MnSO_4$) (Shemesh and Chai, 2013).

Biofilm Formation Assay

A mother liquor containing 1M Cd^{2+} was prepared using cadmium sulfate ($3CdSO_4$-$8H_2O$) and sterilized with a 0.22 μm bacterial filter followed by storage at 4°C.

To analyze the impacts of Cd^{2+} on biofilm formation, we distributed 5 μL of 1JN2 suspension (10^6 CFU/mL) dropwise on each LBGM agar plate containing different Cd^{2+} concentrations, including 0, 1, 2, 3, 4, and 5 mM. The plates were then incubated at 30°C for 72 h (Yang et al., 2018).

Tomato Root Colonization by *Bacillus subtilis* 1JN2

Three treatment categories, A: Water, B: *B.subtilis* 1JN2, and C: *B.subtilis* 1JN2 + Cd^{2+}, were used to detect the colonization ability of tomato plants (obtained from Shanghai Cooperation 903, seed market) by *B. subtilis* 1JN2 after cadmium ion treatment. Each treatment was conducted in three replicates with 20 plants per replicate. Tomato plants with 3-4 euphylla were transferred from seedling trays into experimental pots (10 cm height x 10 cm diameter) filled with 0.5kg of nutrient soil. Each pot was supplied with 20 mL of *B.subtilis* 1JN2 (10^7 CFU/mL) 7 days after transplantation. Thereafter, pots in the treatment C category were supplemented with 20 mL of Cd^{2+} solution (6 mM) 14 days after transplantation. Greenhouse growth conditions included a temperature of 30°C with 16/8 h of light/dark photoperiod.

After treatment, the plant roots were collected 21 days post-transplantation and analyzed using ZEISS LSM 700 after fixation. The colonization ability of 1JN2 was evaluated in treatments B and C using fluorescent analysis described by Yang et al. (2018). The GFP was selected via a Smart Setup, and the excitation and emission wavelengths were 488 nm and 493-550 nm, respectively.

Collection of Cd^{2+}-treated Bacterial Cells

We inoculated 0.5 mL of 1JN2 suspension (10^6 CFU/mL) into 50 mL of LB broth supplemented with 3 mM Cd^{2+} and incubated the cells at 30°C for 24 h. The inoculation was conducted in twelve replicates, among which three replicates each were used for bacterial cells collection at 6, 12, 18, and 24 h after inoculation. Bacterial cells were also collected from a blank LB broth (control) inoculated in triplicate without Cd^{2+} at 24 h post-inoculation. The cell collection was conducted by centrifugation at 5000 rpm for 5 mins, then stored in liquid nitrogen for RNA extraction. The obtained supernatants were used for EPS and γ-PGA content detection.

EPS and γ-PGA Content Detection following 1JN2 Treatment with Cd^{2+}

For EPS detection, we transferred 2 mL of the supernatants into test tubes and added 6 mL of anthrone reagent to each test tube. The solutions were then properly mixed and heated in boiling water for 15 min, followed by cooling in ice water for 15 min. The absorbance of each sample was measured at a wavelength of 625 nm, and their sugar contents were obtained based on the glucose standard curve.

Meanwhile, for γ-PGA detection, 3 mL of methylene blue (color developing solution; 10 mg/L) was added into test tubes containing 3 mL of the supernatants and vortexed for 5 min at 25°C. A wavelength of 664 nm was used for measuring the absorbance of each sample, and the γ-PGA content of the samples was determined based on the γ-PGA standard curve.

RNA Extraction and Preparation

Total RNA was isolated from the collected cells using Tiangen reagent and subsequently purified by QIAGEN RNeasy MINI kit according to the manufacturers' instructions. The RNA quality and quantity were determined at 260 nm wavelength via NanoDrop UV spectroscopy (NanoPhotometer® spectrophotometer, IMPLEN, CA, USA) and analyzed on an RNA 6000 Nano Labchip using 2100 bioanalyzer (Agilent technologies).

Library Preparation for Strand-specific Transcriptome Sequencing

Library preparation was conducted at Genepioneer Biotechnologies Co. Ltd., Nanjing, China, using 3 μg of RNA from each sample based on a protocol by Yang et al. (2019). Illumina sequencing libraries were generated using NEBNext® Ultra™ Directional RNA Library Prep Kit (NEB, USA). Briefly, a random hexamer primer and M-MuLV Reverse Transcriptase (RNase H–) were used for the first cDNA strand synthesis, while the second cDNA strand was synthesized using DNA polymerase I and RNase H. NEBNext Adaptors with hairpin loop structure were ligated to the cDNA fragments after adenylation to prepare for hybridization. The library fragments were then purified using the AMPure XP system (Beckman Coulter, Beverly, USA), and their quality was assessed on the Agilent Bioanalyzer 2100 system (Lei et al., 2018).

Clustering and Sequencing

The samples were index-coded and clustered on a cBot Cluster Generation System using TruSeq PE Cluster Kit v3-cBot-HS (Illumina), according to the manufacturer's instructions. An Illumina Hiseq platform (Cloud Health, Nanjing, China, http://www.chgenomics.com) was then used for library sequencing, and paired-end reads generation.

Data Analysis

The initial raw data obtained in fastq format were processed using in-house Perl scripts. Subsequently, HISAT2 2.0.5 (Zhang et al., 2016) was used for reference genome indexing and aligning clean reads to the reference genome. The reads mapped to each gene were counted using String Tie (Pertea et al., 2016). The FPKM (Fragments Per Kilobase of exon model per Million mapped fragments) of each gene was then calculated based on their length and read counts mapped to the gene (Lei et al., 2018).

Differential expression analysis of the groups was performed using the DESeq R package (1.18.0), while the GOseq R package (with corrected gene length bias) was utilized for Gene Ontology (GO) enrichment analysis of the differentially expressed genes. BLAST software was used to test the statistical enrichment of the differentially expressed genes in KEGG pathways (Li et al., 2016).

Quantitative Real-time PCR Analysis

The expression levels of five selected genes of *B.subtilis* 1JN2 cultured under similar conditions were validated by real-time RT-PCR using an iCyclerMyiQ Real-Time PCR System (Bio-Rad, Hercules, CA). The PCR conditions were set as follows: initial denaturation at 95 °C for 2 mins, followed by 40 cycles of denaturation at 95 °C for 10 s, annealing at 65 °C for 15 s and extension 72 °C for 20 s. Melting curve analysis of the amplicons was performed at the end of each PCR run to ensure that unique products had been amplified.

Results

Cd^{2+} Treatment Changed Biofilm Formation by *B.subtilis* 1JN2

We found that biofilm formation by *B.subtilis* 1JN2 varied with the Cd^{2+} concentration (Figure 1). The biofilm colonies gradually reduced, and their surface became denser with Cd^{2+} concentration. Increasing Cd^{2+} concentration from 0 to 2 mM moderately inhibited biofilm formation by 1JN2; however, Cd^{2+} concentration of 3 mM or higher significantly inhibited biofilm formation by 1JN2. Unlike biofilm formation, there was no significant difference in the growth of 1JN2 in Cd^{2+} concentration of 0 to 2 mM Cd^{2+} (Yang et al., 2018).

The biofilm forms were also affected by Cd^{2+} treatment. Biofilm surfaces of the Cd^{2+}-treated cells were complanate compared to the convex surfaces of the group without Cd^{2+} Moreover, the viscosity of the biofilms also increased with the Cd^{2+} concentration.

Cd^{2+} Treatment Influenced Tomato Roots Colonization by *B.subtilis* 1JN2

Since biofilm formation is an important step in root colonization, it was also imperative to evaluate the effect of Cd^{2+} on the root colonization ability of *B.subtilis* 1JN2. A GFP-tagged 1JN2 was constructed for the root colonization experiment in the greenhouse. The population of *B.subtilis* 1JN2, which colonized the tomato roots, decreased with an increase in Cd^{2+} concentration (Figure 2), indicating that biofilm inhibition caused by Cd^{2+} affected the colonization ability of 1JN2. The colonized position was also changed since many 1JN2 cells were found in tomato root cells compared to the root surface (Figure 2-C). Conversely, many 1JN2 colonies could be seen on the root surface of the group without Cd^{2+}, showing that root surface colonization is important in preventing soil-borne pathogen infections.

RNA Sequencing and Identification of Differentially Expressed Genes (DEGs)

Cell samples were collected at 4-time points (6 h, 12 h, 18 h, and 24 h) after Cd^{2+} treatment. The samples collected at 6 h, 12 h, 18 h, and 24 h were denoted S2, S3, S4, and S5, respectively, while the blank control without Cd2+ was designated S1. The sequence data summary is presented in Table 1. More than 93% of the clean reads from each sample mapped to the reference genome, indicating that the obtained transcriptome data were suitable for further analysis. The raw data were deposited to **NCBI SRA database** with accession number: PRJNA646606 (https://www.ncbi.nlm.nih.gov/search/all/?term=PRJNA646606).

Table 1 Summary of RNA-seq data and the reads mapped to *B.subtilis* 1JN2 genome

Samples	Read Number	Base Number	GC Content	%≥Q30
S1-1	7996483	2398944900	45.09	95.83
S1-2	9237500	2771250000	45.08	96.31
S1-3	10721600	3216480000	44.98	94.94
S2-1	10667725	3200317500	44.49	95.43
S2-2	9264843	2779452900	44.54	93.99
S2-3	9528611	2858583300	44.29	94.29
S3-1	10855623	3256686900	44.37	94.71
S3-2	8856524	2656957200	44.13	94.52
S3-3	9460244	2838073200	44.43	93.75
S4-1	11315033	3394509900	44.59	94.51
S4-2	10009680	3002904000	44.66	94.13
S4-3	9704248	2911274400	44.35	93.06
S5-1	8895735	2668720500	44.68	90.67
S5-2	9932927	2979878100	44.69	93.12
S5-3	9358331	2807499300	44.71	94.85

The number of DEGs between the various time points post Cd^{2+} treatment of *B.subtilis* 1JN2 were analyzed using a Venn diagram (Figure 3a). The number of DEGs between S1 and S2 decreased with the prolongation of treatment time. There were 659 DEGs between S1 and S2, among which 308 were up-regulated, and 351 were down-regulated. However, the number of DEGs between S2 and S3, S3 and S4, S4 and S5 were 178, 36 and 6, respectively (Figure 3b). This implies that the cells undergo an important adjustment phase during the initial period of exposure to Cd^{2+} and later acquire resistance to Cd^{2+} stress. The same trend was observed with the PCA (principal component analysis) results (Figure 3c) which

showed shorter distances between S3, S4, and S5, indicating no significant difference in their gene expression.

Cell Mobility-Related Genes Changed Significantly after Cd^{2+} Treatment

Since Cd^{2+} treatment modified the morphological features of strain 1JN2 biofilm, we checked whether it could also affect the mobility of the strain. The COG (Cluster of Orthologous Groups of Proteins) database is constructed based on the phylogenetic relationship between bacteria, algae, and eukaryotes. Applying BLAST to the database allows for orthologous classification of gene products. The COG (Cluster of Orthologous Groups of Proteins) database BLAST results showed that the most significant changes in gene products of the strain after exposure to Cd^{2+} were related to cell mobility, followed by chromatin structure and dynamics, amino acid and nucleotide transport and metabolism (Figure 4). Moreover, a comparison between S1 and S2 indicated that the strain could perceive and respond to Cd^{2+} stress after some period of exposure via regulatory metabolism. These results are consistent with the observed biofilm morphological changes of the strain.

Flagella Synthesis- and Assembly-related Genes Increased in Strain 1JN2 after Cd^{2+} Treatment

The flagellum is the most important motor organ which plays an important role in the mobility and chemotaxis of bacterial cells. Due to the observed significant effects of Cd^{2+} on the strain's mobility, we assessed its effects on flagella encoding and assembly genes. KEGG (Kyoto Encyclopedia of Genes and Genomes) is a database for systematic gene function analysis and genomic information. The significant pathway enrichments can indicate the main biochemical, metabolic, or signal transduction pathways associated with differentially expressed genes. According to KEGG analysis, flagella encoding and assembly genes were significantly enhanced than the control group 12 hours after Cd^{2+} treatment (Figure 5). The differential genes at the later sampling time points were mainly involved in metabolic-related reactions, such as glycolysis/gluconeogenesis and biosynthesis of valine, leucine, isoleucine, pantothenate, and CoA. Figure 6 also illustrates similar results.

Effect of Cd^{2+} on the Extracellular Secretions of Strain 1JN2

We evaluated the effects of Cd^{2+} stress on the extracellular secretions (polysaccharides and proteins) of strain 1JN2 and found that the extracellular protein-related genes (*tapA-sipW-tasA*) were not expressed in the strain. However, the expression of EPS encoding genes (*epsA-O*) decreased significantly after Cd^{2+} treatment, indicating that Cd^{2+} reduces polysaccharides levels in *B. subtilis* 1JN2 biofilm (Figure 7). According to Yu et al. (2016), γ-PGA plays an important role in the polymorphism of *B. Subtilis* biofilm; therefore, we assessed the expression of the γ-PGA encoding genes in this study. Moreover, the genes encoding γ-PGA (*pgsB-pgsC-pgsA*) were highly expressed after Cd^{2+} treatment, but there was no significant difference in the expression at the last four sampling time points. This indicated that changes in the extracellular secretions mainly occurred within a certain period after 1JN2 exposure to Cd^{2+} treatment. Similar results were obtained by comparing the changes in EPS and γ-PGA levels at different

time points after Cd^{2+} treatment. The EPS levels remained unchanged at very low concentrations, while γ-PGA content increased significantly compared to the control group (Figure 8).

Additionally, studies have reported that surfactants secretion by *Bacillus* increases after exposure to cations, thus, we evaluated the expression of surfactin-encoding genes. The expression levels of the genes related to the surfactin-related genes (*srfAA-srfAB-srfAC*) were also significantly increased following Cd^{2+} treatment (Figure 7).

Effect of Cd^{2+} on the Regulation Pathway of 1JN2 Biofilm Formation

According to related reports, multiple histidine kinases (KinA, KinB, KinC, KinD, and KinE) mainly sense exogenous environmental signals and collectively act on Spo0A either directly through protein phosphorylation or indirectly via a Phospho-relay (Mcloon et al., 2011). We examined the expression of the regulatory factors of the biofilm formation pathway of 1JN2 and found that the expression of *kinC* significantly increased after exposure to Cd^{2+}, reaching its highest level at 24 h (Figure 7). This shows that KinC plays an important role in detecting the change in exogenous ion signals. It has been reported that KinC induces low levels of Spo0A-P in response to potassium cations evacuation caused by surfactin-generated pores in *B.subtilis* membrane (Lopez et al., 2009). But the main regulatory factor showed a downward trend. Therefore, increased kinC levels reduced the expression of Spo0A after exposure to Cd^{2+} (Figure 7). To explain this, we also examined the changing trends of Sda and DnaA encoding genes following Cd^{2+} treatment. Sda is a critical protein that controls the sporulation or biofilm states in bacterial cells. It can prevent the transfer of phosphate groups from histidine kinase to Spo0F, thereby blocking or delaying Spo0A activity (Whitten et al., 2007; Yan et al., 2016). The replication initiation protein, DnaA, activates *sda*, which effectively prevents phosphate group accumulation and activates Spo0A, thereby preventing cells from premature sporulation stage (Burkholder et al., 2001). Sda expression and activity are reduced when the cell enters the stationary phase, therefore, reversing the Spo0A and proteolytic activities of the existing Sda protein (Ruvolo et al., 2006). Thus, the increased expression levels of *dnaA* and *sdaAB* after exposure to Cd^{2+}may have led to the changes in Spo0A. Meanwhile, the two-component regulatory system SinI/SinR limited the production of extracellular polysaccharides, similar to the effects of increased expression of AbrB encoding genes after Cd^{2+} treatment.

We also evaluated the changes in the γ-PGA regulatory factors and found that SigD significantly increased after Cd^{2+} treatment. This activated the expression of flagella encoding and assembly genes by regulating γ-PGA production through another two-component regulatory system called DegU/S. The components of this regulatory pathway (*sigD*, *degS*, and *degU*) increased consistently, resulting in γ-PGA production, which in turn enhanced the mobility of the strain. The changes in the expression levels of γ-PGA and EPS are consistent with the previously reported switch-like mechanism (Yu et al., 2016).

Real-time PCR Validation of the Selected DEGs

Five genes were selected for qPCR assay to confirm the reproducibility and accuracy of the transcriptome data. We found less variation between the two data sets from RNA-seq and RT-PCR analyses (Figure 9).

Discussion

Biofilms play important roles in the life cycle of *Bacilli* (Branda et al., 2001; Vlamakis et al., 2013), such as protection from antibiotics (Høiby et al., 2010) and adherence to the surface of objects. *Bacillus* is a preferable biocontrol agent of plant pathogens because of its strong survivability; therefore, various *Bacillus* species have been screened from the laboratory and applied in the field (Chen et al., 2012). Colonization is a very important factor in biocontrol efficacy since the level of colonization directly affects the inhibition capacity of biocontrol agents (Chen et al., 2012). Various factors such as light, pH, and metal ions affect the colonization ability of biocontrol strains in the field. These factors also represent bottlenecks limiting the application of laboratory-generated biocontrol strains in the field.

Among the main components of *Bacillus* biofilm, EPS and γ-PGA help the strain colonize the host roots, thus inhibiting plant pathogens effectively (Yu et al., 2016). Wild-type *Bacillus* species exhibit different biofilm morphologies due to differences in their extracellular secretions. Moreover, the role of these components in biofilm formation and morphological changes have been demonstrated using deletion mutants of different extracellular secretory components (Yan et al., 2016; Yu et al., 2016). We found that Cd^{2+} can change the morphology of *B. subtilis* 1JN2. High Cd^{2+} concentrations increased the viscosity and flattened the surface of the 1JN2 biofilm, showing that exogenous heavy metal ions can affect the composition of the extracellular secretion of the strain. This study evaluated the mechanisms involved in the extracellular component change and determined whether the biological functions of the strain are affected by the change.

Since *B. subtilis* 1JN2 has proven to be a significant biocontrol agent against *Ralstonia* via host colonization (Yang et al., 2012), we assessed whether the biofilm morphological changes caused by Cd^{2+} impact the colonization ability of this strain. The results show that the change in extracellular components caused by Cd^{2+} treatment reduced tomato root colonization by the strain. However, the effect of Cd^{2+} on the biocontrol efficiency of *B. subtilis* 1JN2 against *Ralstonia* was not significant. Therefore, we further explored the mechanism involved in the biofilm changes caused by Cd^{2+} treatment.

The transcriptome sequencing results show that the expression level of the EPS encoding genes significantly reduced, but that of γ-PGA genes increased after Cd^{2+} treatment. Further analysis revealed that KinC is the receptor of exogenous Cd^{2+} in *B. subtilis* 1JN2, which activates the main regulatory factor Spo0A through phosphorylation. This activation process is regulated by the critical protein Sda, which also controls sporulation or biofilm formation in bacterial cells. The decline in Spo0A levels inhibited the EPS synthesis through the SinI/SinR two-component regulatory system and increased AbrB levels.

Cadmium ion treatment significantly increased the expression of SigD, thus enhancing the expression of the flagella encoding and assembly genes of the strain. This further activated the DegS/DegU two-

component regulatory system for γ-PGA production, enhancing the mobility of the strain and conversion of EPS to γ-PGA. Both EPS and γ-PGA have been reported to improve the colonization ability of the 1JN2, which may be why the biocontrol effect of the strain against *Ralstonia* did not reduce after Cd^{2+} treatment. Essentially, the roles of γ-PGA and EPS in 1JN2 colonization are interchangeable.

The expression of surfactin synthesis-related genes was also significantly increased after Cd^{2+} treatment. A previous study also reported that metal ions could induce surfactants secretion by *Bacillus* (Lopez et al., 2009). Increased surfactin levels improve the biocontrol ability of the strain by resisting the metal ion stress and exerting inhibitory activity against *Ralstonia solanacearum* (Almoneafy et al., 2014).

Generally, the main changes caused by Cd^{2+} treatment in *Bacillus subtilis* 1JN2 biofilm were EPS content, increased γ-PGA and surfactin levels, and enhanced cell mobility. Based on this, we deduce that the adaptive changes by *Bacillus* do not affect its inherent colonization and disease control activity within a certain range of cadmium ion concentration. Through surfactin secretion, *B. subtilis* can alleviate pathogen infections and heavy metal stress for the host plant. Exploring additional mechanisms involved in *B. subtilis* biofilm changes and screening of multifunctional biocontrol strains will be the focus of our future work.

Abbreviations

EPS: extracellular polysaccharides;

γ-PGA: poly-γ-glutamic acids;

FPKM: fragments per kilobase of exon model per million mapped fragments.

Declarations

Ethics approval and consent to participate

Not applicable.

Consent for publication

Not applicable.

Availability of data and material

The raw data were deposited to **NCBI SRA database** with accession number: PRJNA646606 (https://www.ncbi.nlm.nih.gov/search/all/?term=PRJNA646606).

Competing interests

The corresponding author states that there is no conflict of interest on behalf of all authors.

Funding

This work was funded by the Natural Science Foundation for Higher Education Institutions of Jiangsu Province (21KJA210005), Natural Science Foundation of Jiangsu Province (BK20170467), and Jiangsu University Student Innovation Training Program (201910323013Z). These funding bodies had no role in the design of the study and collection, analysis, and interpretation of data and in writing the manuscript.

Authors' contributions

Investigation: Wei Yang, Haixia Yan, Guanghui Dong, Zhengpeng Li, Chunhao Jiang, Dalu Gu, Dongdong Niu, and Danni Zhou. Methodology: Dongdong Niu and Yuming Luo. Writing original draft: Wei Yang. Review and editing: Yuming Luo.

Acknowledgements

We appreciated Genepioneer Biotechnologies Co. Ltd. Nanjing, China, for the help in data analysis.

References

1. Almoneafy AA, Kakar KU, Nawaz Z et al (2014) Tomato plant growth promotion and antibacterial related-mechanisms of four rhizobacterial *Bacillus* strains against *Ralstonia solanacearum* [J]. Symbiosis 63(2):59–70
2. Ashiuchi M, Misono H (2002) Biochemistry and molecular genetics of poly-γ-glutamate synthesis [J]. Appl Microbiol Biotechnol 59(1):9–14
3. Bais HP, Fall R, Vivanco JM (2004) Biocontrol of *Bacillus subtilis* against infection of Arabidopsis roots by *Pseudomonas syringae* is facilitated by biofilm formation and surfactin production [J]. Plant Physiol 134(1):307–319
4. Beauregard PB, Chai Y, Vlamakis H et al (2013) *Bacillus subtilis* biofilm induction by plant polysaccharides [J]. Proc Natl Acad Sci USA 110(17):1621–1630
5. Branda SS, Gonzálezpastor JE, Benyehuda S et al (2001) Fruiting body formation by *Bacillus subtilis* [J]. Proc Natl Acad Sci USA 98(20):11621–11626
6. Burkholder WF, Kurtser I, Grossman AD (2001) Replication initiation proteins regulate a developmental checkpoint in *Bacillus subtilis* [J]. Cell 104(2):269–279
7. Chai Y, Norman T, Kolter R et al (2011) Evidence that metabolism and chromosome copy number control mutually exclusive cell fates in *Bacillus subtilis* [J]. EMBO J 30(7):1402–1413
8. Chen Y, Cao S, Chai Y et al (2012) A *Bacillus subtilis* sensor kinase involved in triggering biofilm formation on the roots of tomato plants [J]. Mol Microbiol 85(3):418–430
9. Chen Y, Yan F, Chai Y et al (2013) Biocontrol of tomato wilt disease by *Bacillus subtilis* isolates from natural environments depends on conserved genes mediating biofilm formation [J]. Environ Microbiol 15(3):848–864

10. Hamon MA, Lazazzera BA (2001) The sporulation transcription factor Spo0A is required for biofilm development in *Bacillus subtilis* [J]. Mol Microbiol 42(5):1199–1209
11. Høiby N, Bjarnsholt T, Givskov M et al (2010) Antibiotic resistance of bacterial biofilms [J]. Int J Antimicrob Agents 35(4):322–332
12. Lei Z, Wu Y, Nie W et al (2018) Transcriptomic analysis of xylan oligosaccharide utilization systems in *Pediococcus acidilactici* strain BCC-1 [J]. J Agric Food Chem 66(18):4725–4733
13. Li Y, Zhang W, Chang L et al (2016) Vitamin C alleviates aging defects in a stem cell model for Werner syndrome [J]. Protein Cell 7(7):478–488
14. Liu J, He D, Li XZ et al (2010) Gamma-polyglutamic acid (gamma-PGA) produced by *Bacillus amyloliquefaciens* C06 promoting its colonization on fruit surface [J]. Int J Food Microbiol 142(1):190–197
15. López D, Fischbach MA, Chu F et al (2009) Structurally diverse natural products that cause potassium leakage trigger multicellularity in *Bacillus subtilis* [J]. Proc Natl Acad Sci USA 106(1):280–285
16. Mcloon AL, Kolodkin-Gal I, Rubinstein SM et al (2011) Spatial regulation of histidine kinases governing biofilm formation in *Bacillus subtilis* [J]. J Bcteriology 193(3):679–685
17. Morikawa M, Kagihiro S, Haruki M et al (2006) Biofilm formation by a *Bacillus subtilis* strain that produces gamma-polyglutamate [J]. Microbiology 152(9):2801–2807
18. Ogunleye A, Bhat A, Irorere VU et al (2015) Poly-γ-glutamic acid: production, properties and applications [J]. Microbiology 161(1):1–17
19. Pertea M, Kim D, Pertea GM et al (2016) Transcript-level expression analysis of RNA-seq experiments with HISAT, StringTie and Ballgown [J]. Nat Protoc 11(9):1650–1667
20. Poo H, Park C, Kwak MS et al (2010) New biological functions and applications of high-molecular-mass poly-gamma-glutamic acid [J], vol 7. Chemistry & Biodiversity, pp 1555–1562. 6
21. Ruvolo MV, Mach KE, Burkholder WF (2006) Proteolysis of the replication checkpoint protein Sda is necessary for the efficient initiation of sporulation after transient replication stress in *Bacillus subtilis* [J]. Mol Microbiol 60(6):1490–1508
22. Shemesh M, Chai Y (2013) A combination of glycerol and manganese promotes biofilm formation in *Bacillus subtilis* via histidine kinase KinD signaling [J]. J Bacteriol 195(12):2747–2754
23. Stanley NR, Lazazzera BA (2005) Defining the genetic differences between wild and domestic strains of *Bacillus subtilis* that affect poly-gamma-dl-glutamic acid production and biofilm formation [J]. Mol Microbiol 57(4):1143–1158
24. Ursu I, Craciun V, Mihailescu IN et al (1989) Molecular characterization and protein analysis of the cap region, which is essential for encapsulation in *Bacillus anthracis* [J]. J Bacteriol 171(2):722
25. Vlamakis H, Chai Y, Beauregard P et al (2013) Sticking together: building a biofilm the *Bacillus subtilis* way [J]. Nat Rev Microbiol 11(3):157–168

26. Whitten AE, Jacques DA, Hammouda B et al (2007) The Structure of the KinA-Sda complex suggests an allosteric mechanism of histidine kinase inhibition [J]. J Mol Biol 368(2):0–420
27. Xue QY (2008) Studies on screening strategy of antagonists against *Ralstonia solanacearum* and biocontrol mechanism of antagonistic strain xy21 [D]. Nanjing Agricultural University
28. Yan F, Yu YY, Wang LY et al (2016) The *comER* gene plays an important role in biofilm formation and sporulation in both *Bacillus subtilis* and *Bacillus cereus* [J]. Front Microbiol 7:1025
29. Yang YW, Mi JD, Liang JD et al (2019) Changes in the carbon metabolism of *Escherichia coli* during the evolution of Doxycycline resistance [J]. Front Microbiol 10:2506
30. Yang W, Xu Q, Liu HX et al (2012) Evaluation of biological control agents against *Ralstonia* wilt on ginger [J]. Biol Control 62(3):144–151
31. Yang W, Yan HX, Wang JL et al (2015) Selection of a *Bacillus subtilis* strain alleviating Cd^{2+} stress in host plants and the mechanism [J]. Jiangsu J Agricultural Sci 31(4):806–
32. Yang W, Yan HX, Zhang J et al (2018) Inhibition of biofilm formation by Cd^{2+} on *Bacillus subtilis* 1JN2 depressed its biocontrol efficiency against *Ralstonia* wilt on tomato [J]. Microbiol Res 215:1–6
33. Yu YY, Yan F, Chen Y et al (2016) Poly-γ-glutamic acids contribute to biofilm formation and plant root colonization in selected environmental isolates of *Bacillus subtilis* [J]. Front Microbiol 7(e14653):1811
34. Zhang Y, Chen S, Hao X et al (2016) Transcriptomic analysis reveals adaptive responses of an *Enterobacteriaceae* Strain LSJC7 to arsenic exposure [J]. Front Microbiol 7:636

Figures

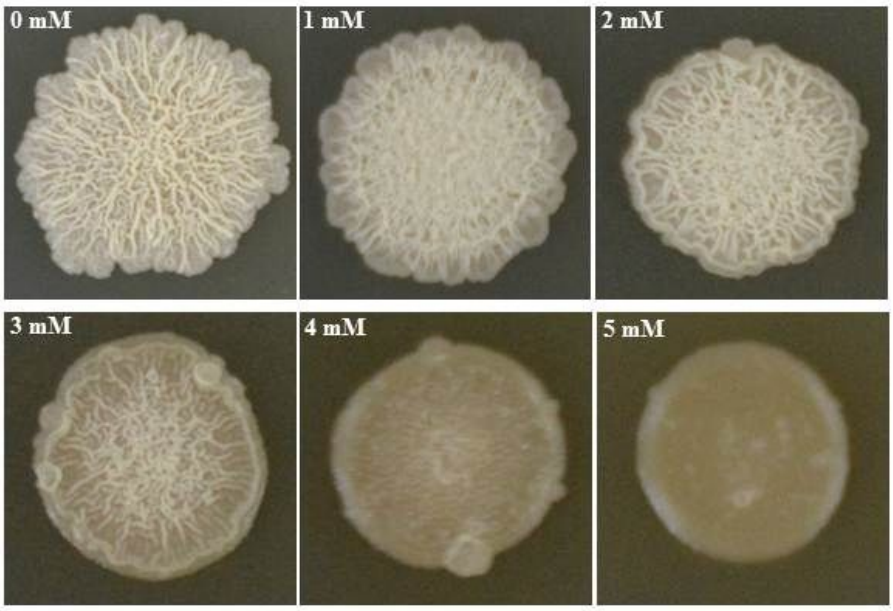

Figure 1

Impacts of Cd^{2+} on the biofilm colonies of *B.subtilis* 1JN2. 5 ul of 1JN2 suspension (10^6 CFU/mL) was spotted on the surface of LBGM agar plate with a Cd^{2+} gradient of 0, 1, 2, 3, 4 and 5 mM, the picture was taken at 72h post incubation at 30℃.

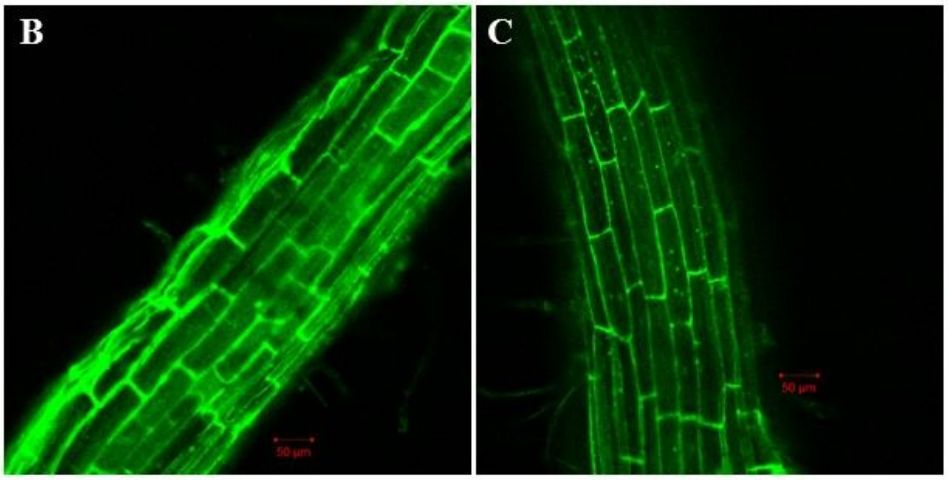

Figure 2

Confocal microscope detection of *B.subtilis* 1JN2 on the root of tomato with (C) or without (B) Cd^{2+} treatment. Fluorescent analysis was carried out using ZEISS LSM 700. GFP was selected in Smart Setup, the excitation wavelength is 488nm, and the emission wavelength is 493-550nm.

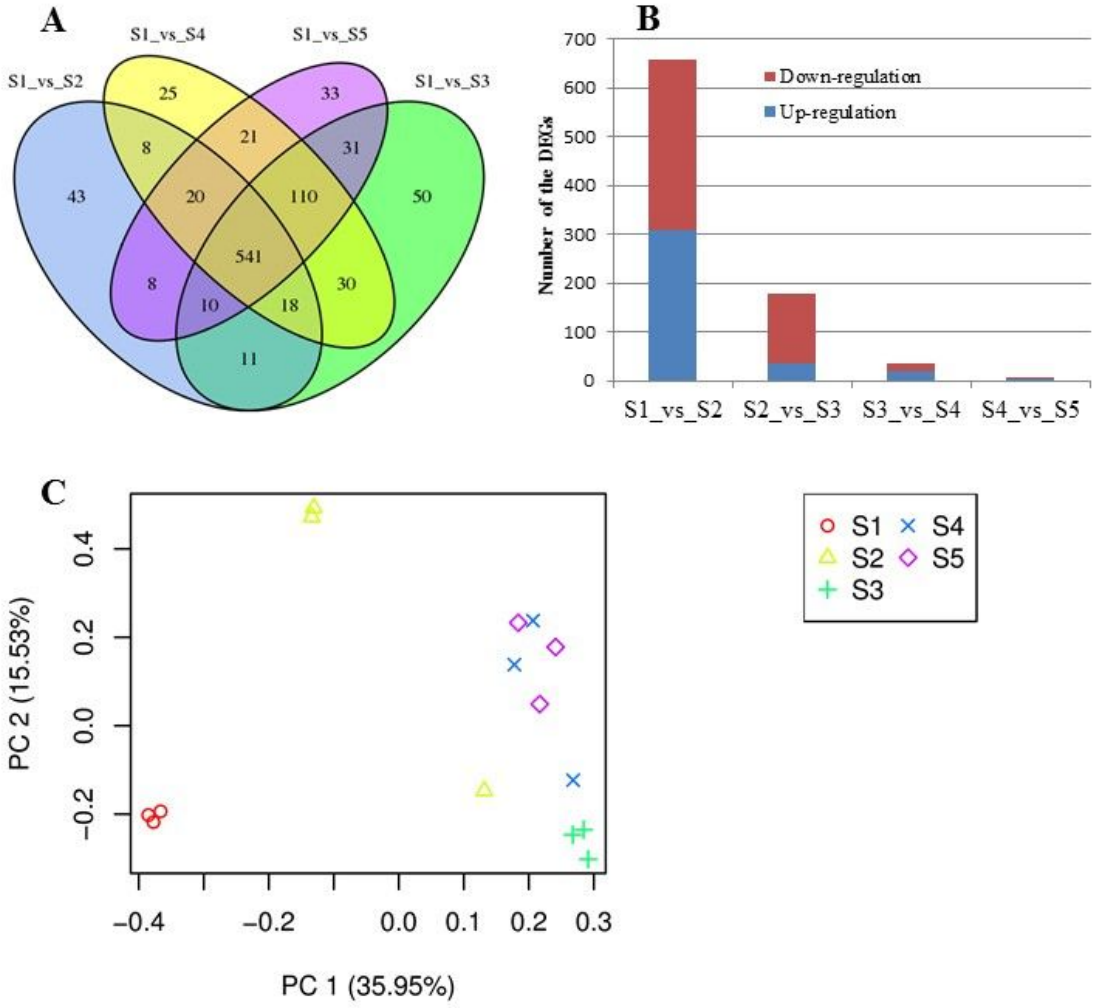

Figure 3

Analysis of the differentially expressed genes of *B.subtilis* 1JN2 after Cd^{2+} treatment. A: Venn diagram analysis, B: numbers of DEGs between time points, C: PAC analysis. Samples collected at 6h, 12h, 18h, and 24h were named as S2□S3□S4□S5 and the blank control that without Cd^{2+} was named as S1. Comparison between S1 and S2 means the DEGs between the two samples, and so on.

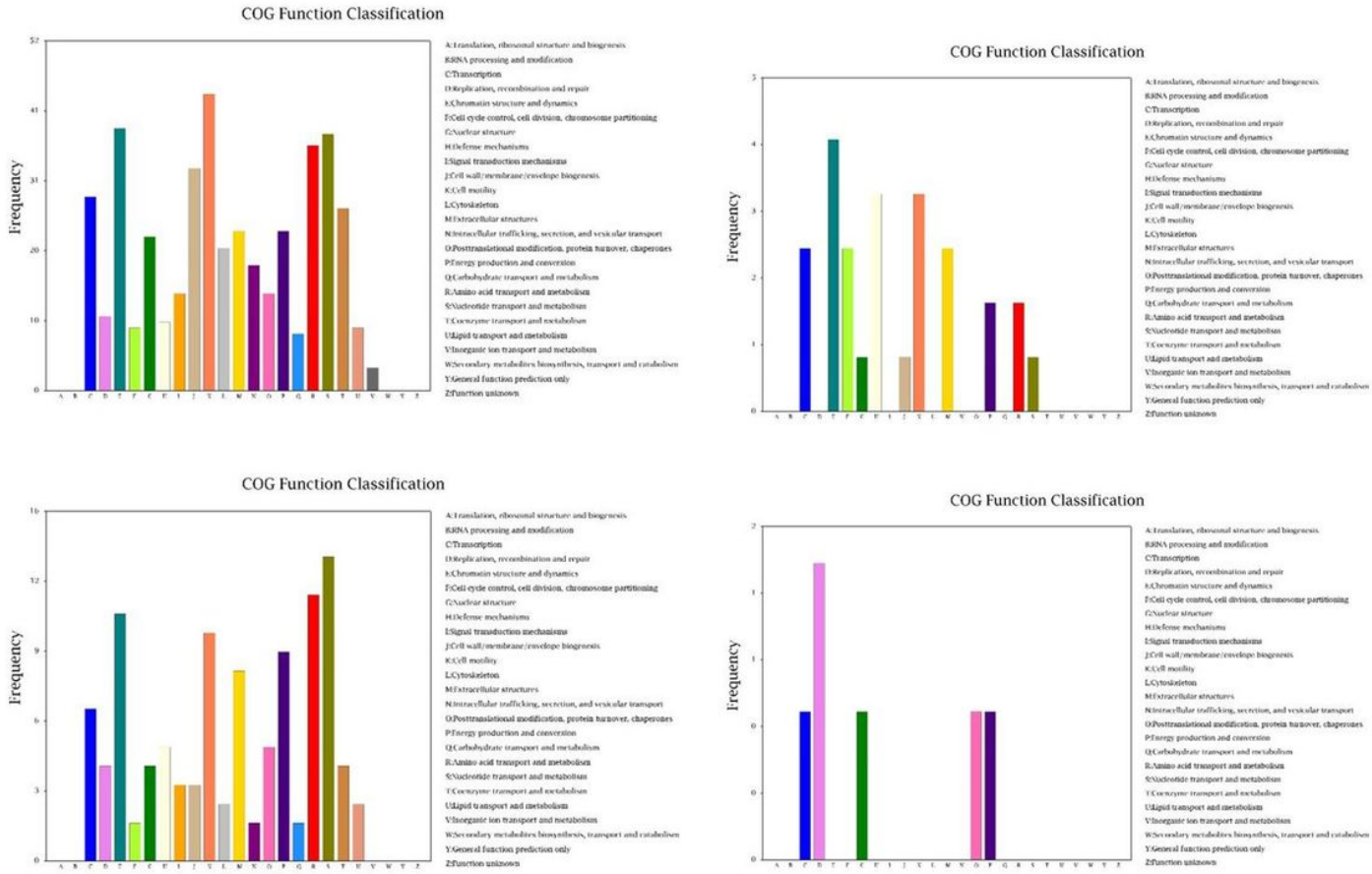

Figure 4

COG (Cluster of Orthologous Groups of Proteins) function classification of the DEGs of *B.subtilis* 1JN2 after Cd^{2+} treatment. A, B, C and D means the comparison of DEGs according to COG function classification between S1 and S2, S2 and S3, S3 and S4, S4 and S5 separately.

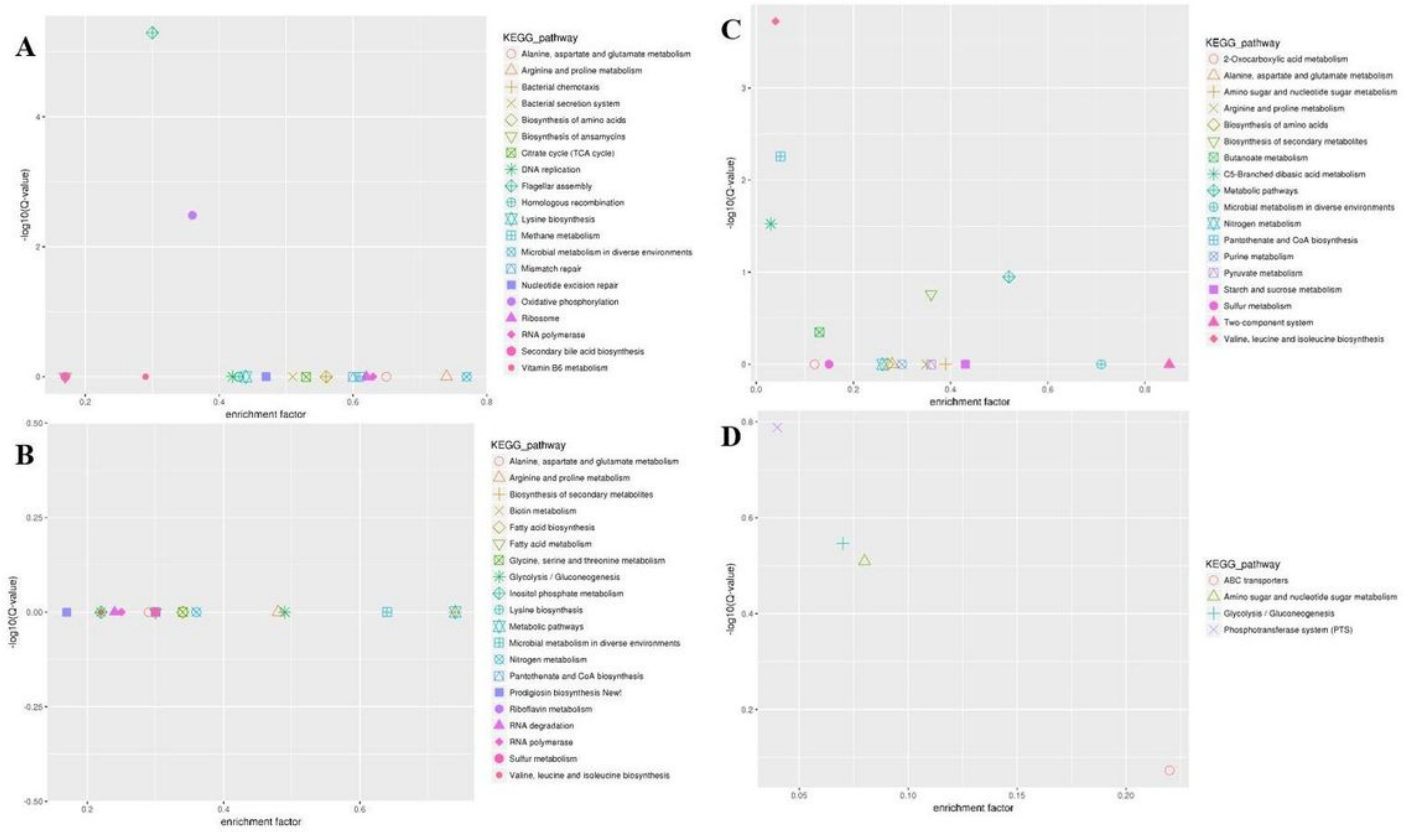

Figure 5

Scatter plot of KEGG (Kyoto Encyclopedia of Genes and Genomes) pathway enrichment of the DEGs of *B.subtilis* 1JN2 after Cd^{2+} treatment. A, B, C and D means the comparison of DEGs according to KEGG pathway enrichment between S1 and S2, S2 and S3, S3 and S4, S4 and S5 separately.

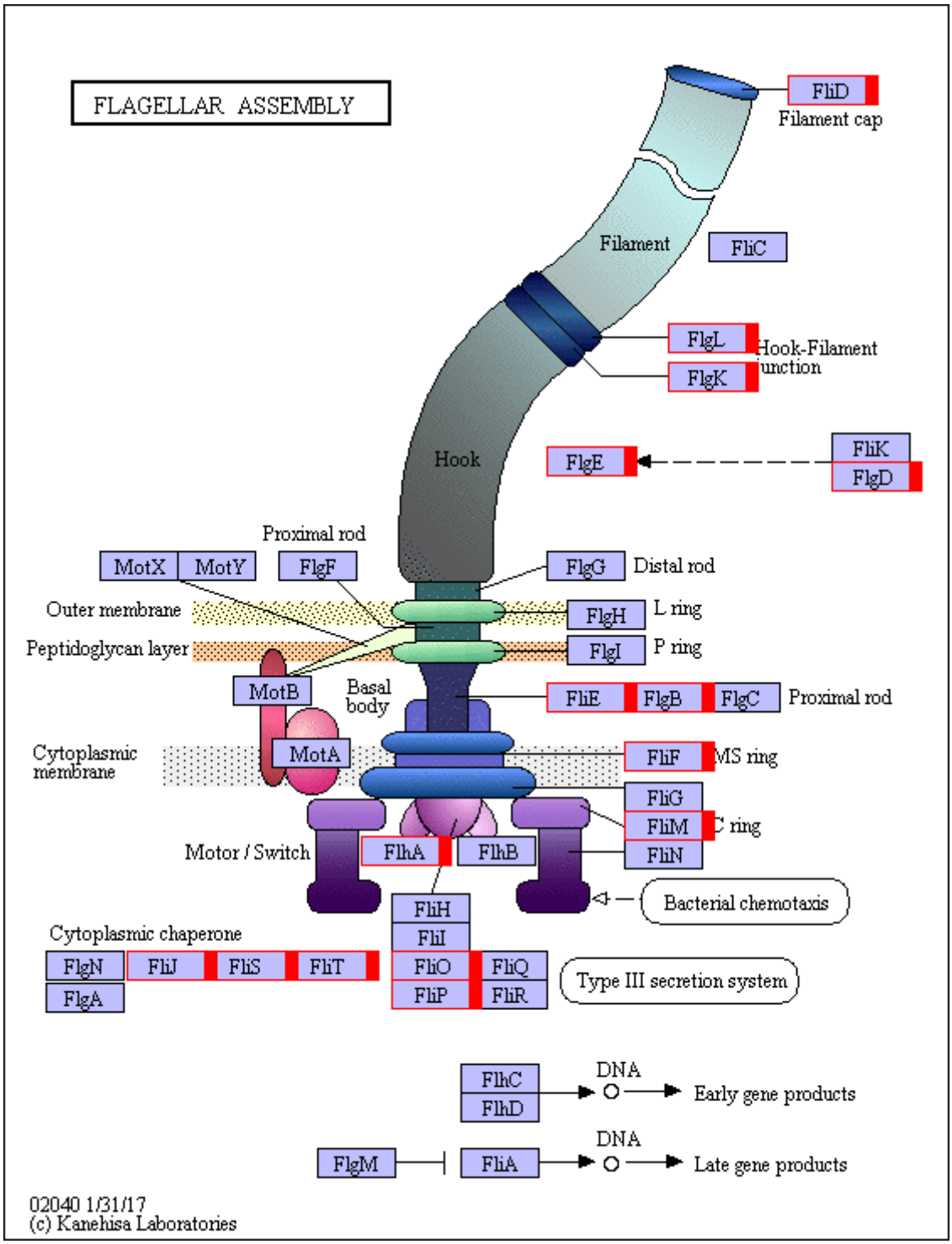

Figure 6

KEGG (Kyoto Encyclopedia of Genes and Genomes) pathway annotation of the genes involved in flagella encoding and assembly of *B.subtilis* 1JN2 after Cd^{2+} treatment. Genes markered with red indicate up-regulation.

Figure 7

Relative expression level of the genes involved in extracellular secretion and regulation of *B.subtilis* 1JN2 after Cd^{2+} treatment. The histogram was based on the expression level in FPKM (Fragments per Kilobase of Transcript per Million Fragments Mapped) value.

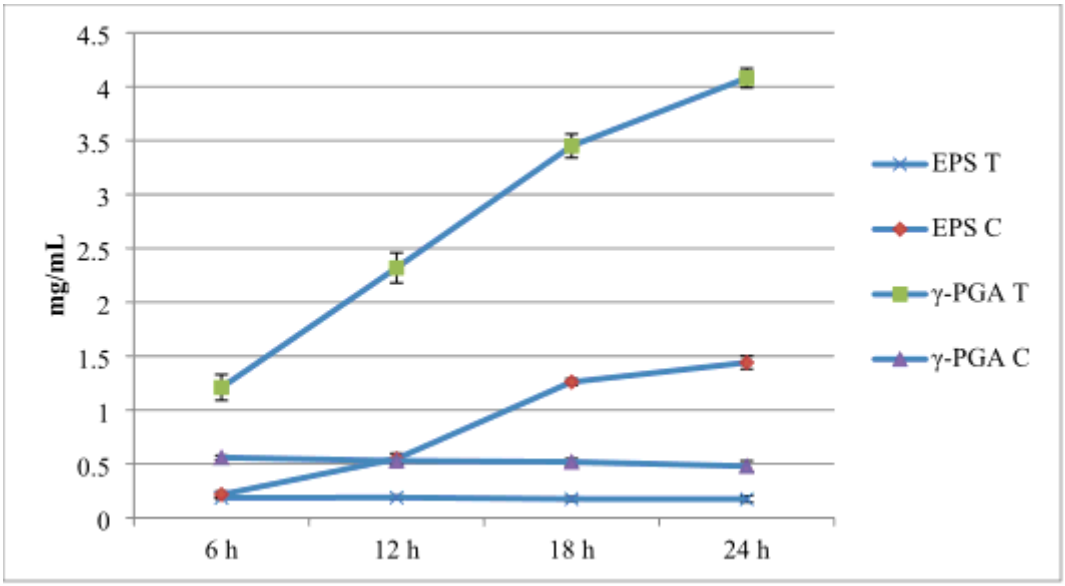

Figure 8

The content of EPS and γ-PGA of the strain 1JN2 after Cd^{2+} treatment. 3mM Cd^{2+} was added in the broth and the supernatants at 6、12、18 and 24h after inoculation were used to detect the content of EPS and γ-PGA. T means treated with Cd^{2+} and C means control without Cd^{2+}.

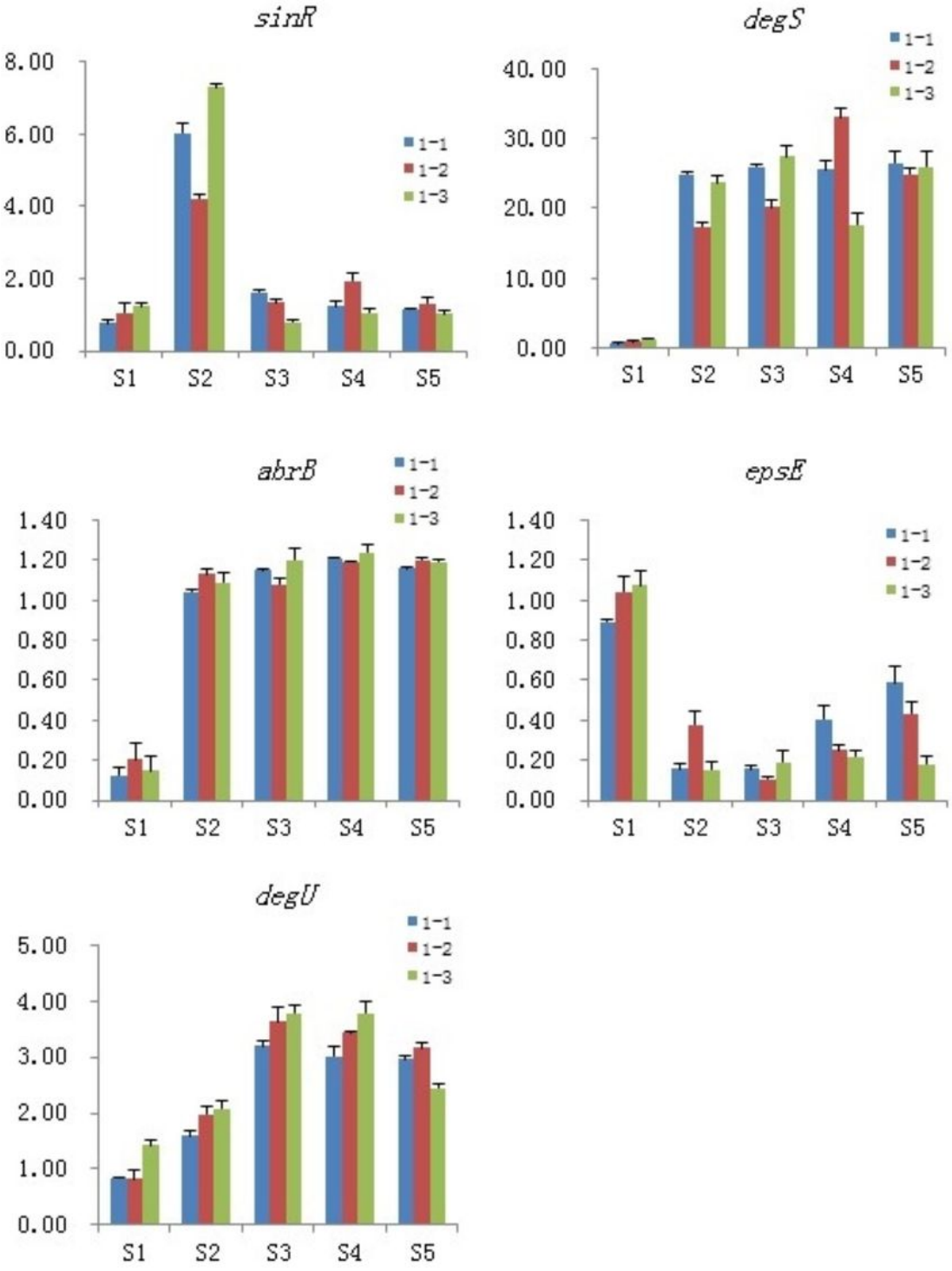

Figure 9

Validation of the selected DEGs by real-time PCR. Samples collected at 6h, 12h, 18h, and 24h were named as S2、S3、S4、S5 and the blank control that without Cd^{2+} was named as S1, 1-1, 1-2 and 1-3 means the three replicates of each sample.